Umudike Journal of Engineering and Technology (UJET); Vol. 9, No. 1, June 2023, pp. 55 – 69; Michael Okpara University of Agriculture, Umudike, Print ISSN: 2536-7404, Electronic ISSN:2545-5257; http://ujetmoua.com; https://doi.org/10.33922/j.ujet_v9i1_7

SHEA BUTTER OIL TRANSESTERIFICATION VIA CLAY DOPED BARIUM CHLORIDE CATALYST; RESPONSE SURFACE METHODOLOGY AND GENETIC ALGORITHM EVALUATION

[1]Nwosu-Obieogu K., [2]Onukwuli D. O., [3]Ezeugo J., [1]Ude C. N.

[1]Department of Chemical Engineering, College of Engineering and Engineering Technology, Michael Okpara University of Agriculture, Umudike, Nigeria. (Email: kenenwosuobie@mouau.edu.ng)

[2]Department of Chemical Engineering, College of Engineering and Engineering Technology, Nnamdi Azikiwe University Awka, Nigeria.

[3]Department of Chemical Engineering, Chukwuemeka Odumegwu University, Uli, Nigeria.

ABSTRACT

A novel clay-doped BaCl (CD-BaCl) heterogeneous catalyst was developed through calcinations at 600^{o}C for four hours and successfully applied for biodiesel production from shea butter oil. The catalyst was characterized by Fourier Transform Infrared Spectroscopy (FT-IR), Scanning Electron Micrograph (SEM), X-ray Diffraction (XRD), X-ray Fluorescence (XRF), and Brunauer-Emmett-Teller(BET) before and after treatment to ascertain its suitability for the process. The shea butter oil was characterized using FT-IR and GC-MS (Gas Chromatography Mass Spectrometer) to confirm its potential for the transesterification process. Response surface methodology (RSM) and Genetic Algorithm (GA) were used to compare the best operating conditions; GA outperformed RSM with a biodiesel yield (81.49%) obtained at a catalyst loading (3 wt%), methanol/molar ratio (12:1 mol/mol), time (3 hours), temperature (50^{o}C), and agitation speed (208.8 rpm). The second-order polynomial model is shown in the (Analysis of Variance) ANOVA with an R^2 value of 0.9981, Adj R^2 (0.9946), and Pred R^2 (0.9499), demonstrating the model's acceptance. The shea butter biodiesel produced complied with ASTM D6751 requirements. As a result, this study showed that GA is more predictive than RSM.

Keywords: *RSM, GA, shea butter, transesterification, biodiesel*

1.0 INTRODUCTION

The reliability of biobased energy resources is essential for economic development as it encourages environmental friendliness, cost-effectiveness, material renewability, and the release of non-toxic pollutants to the environment(Mostafa Marzouk *et al*., 2021; Nazir *et al*., 2021; Esonye *et al*.,2019). Vegetable oil, animal fats, animal dung, and plant waste are viable feedstock depending on the biofuel generated. Due to its synthesis from widely available feedstock, biodiesel is one of the most prevalent biofuels. It is a renewable, sustainable fuel from long-chain fatty acid monoalkyl ester generated from lipid feedstock, such as vegetable oils (Tamoradi et al., 2021; Onukwuli & Ude, 2018).

Shea butter is extracted from the shea nut of the sub-Saharan African shea tree with a high free fatty acid content and is regarded as a partially edible vegetable oil (Abnisa et al., 2021). It has prompted the shea market to develop quickly and is widely used in cosmetics. According to reports from Alaba et al. (2015) and Ajala et al. (2018), it includes unsaturated triglyceride, which qualifies it as a transesterification-friendly substance.

Biodiesel is produced via a transesterification process with a catalyst. A catalyst improves biodiesel yield through a reaction rate increase. Recently, heterogeneous catalysts have been considered for the synthesis of biodiesel because it encourages the reusability of the catalyst, high activity of the catalyst, and high yield(Nisar *et al*., 2021; Taipabu *et al*., 2021).

The catalytic properties of clay are considered during transesterification due to its porosity, high surface area, stability, and desired pore size distribution properties (Jalalmanesh et al., 2021; Salmasi et al., 2020).Several researchers have reported the need to modify the clay via acid/alkaline activation or dope it with new material to improve its properties; Ude and Onukwuli, (2019) developed alkaline activated clay catalyst for gmelina seed oil transesterification. Marques de Costa (2021) transesterified cotton oil with methanol using bentonite, using a solid catalyst developed from clay. Their observation proved that modified/doped clay catalysts are good candidates for transesterification.

Barium Chloride (BaCl) was chosen to dope with clay in this study to improve its catalytic properties. Hence few researchers have reported on applying clay-doped Barium Chloride (CD-BaCl) for oil transesterification. Olutoye et al. (2016) synthesized a barium-modified montmorillonite K10 catalyst for waste cooking transesterification; a biodiesel yield of 83.38% was obtained at 3.5wt.% catalyst loading,

temperature of 150^{o}C , methanol to oil molar ratio of 12:1 and a reaction time of five hours, Yusuf et al. (2021) developed barium- modified zeolite catalyst for waste frying oil transesterification, a biodiesel yield of 93.17% was gotten at 3 wt.% catalyst loading, methanol to oil molar ratio (12:1), temperature (65.38^{o}C) and 2 hours reaction time. Their results proved that doping the clay enhanced the biodiesel yields from the oils.

Studies on improving process parameters utilizing the design of experiments have improved due to the quest for optimal conditions of the biodiesel production process. A statistical design method known as "response surface methodology" allows for evaluating a response prediction model's linear, interactional, and quadratic effects. It implements a box/behnken/central composite design to identify each factor's significance and screen a broad range of variables.

Application of RSM in the transesterification process of shea butter has been reported by Olatunji et al. (2021) on the maximizing of biodiesel yield from shea butter transesterification process using calcined water pod catalyst, a biodiesel yield of 92% was obtained at 55 minutes, 3:1 (w/w) methanol/oil ratio and catalyst loading of 2.5g; a higher optimization algorithm referred to as genetic algorithm which dwells on biological evolution, compares the optimal condition of the transesterification process with RSM. To the best of our knowledge, RSM and GA comparison has not been carried out on shea butter oil transesterification using CD-BaCl catalyst; the works bridge the lacuna by developing a CD-BaCl catalyst for shea butter oil transesterification and optimizing the process using RSM and GA techniques.

2.0 MATERIALS AND METHODS

2.1 Materials

The shea butter was purchased from National Research Institute, Umudike. Clay was chosen for the catalyst preparation because of its availability. Barium chloride used for impregnation of the clay and methanol were purchased from Sigma-Aldrich, Poole, England.

2.2 Apparatus

250ml three-necked flat bottom flask, 500ml round bottom flask, glass beads, thermometers, plastic rod stirrers, hot plate magnetic stirrer, 100ml storage containers, a condensation unit, distillation unit, funnels, burettes (50ml), conical flasks (250ml), conical flasks (1L), 500ml beakers, measuring cylinders (250, 500 and 1000ml each), a stopwatch and 1L separating funnels for separating glycerol and biodiesel phases.

2.3 Characterization of the Oil

The shea butter oil was characterized using the American Society for Testing Material (ASTM) standard for physiochemical properties (Dai et al., 2021; Sahu, 2021; Yatish et al., 2021)and instrumentation such as FTIR (Shimadzu FTIR-8400S) and GC–MS were used to evaluate the functional group and fatty acid profile of the oil respectively (Bambase et al., 2021; Lim et al., 2020; Naveenkumar & Baskar, 2021)

2.4 Synthesis of barium chloride doped clay catalyst

10% barium chloride solution was mixed with the prepared clay sample and allowed to stand overnight. The mixture was dried in a hot air oven at 105 ^{o}C and calcinated in a muffle furnace at 600 ^{0}C for four hours. The product was kept in an airtight sample holder (Dadhania et al., 2021).

2.5 Characterization of the clay sample

The ASTM D4067 (1986) method was used to characterize the raw and doped clay samples in order to determine their physiochemical properties, the functional group using a Fourier transform infrared spectrometer, the morphology using a scanning electron microscope, and the mineralogy/type of the clay using an X-ray diffractometer.

2.6 Acid-catalyzed esterification of shear butter oil

One thousand grams (1000g) of shear butter oil was preheated at 60 ^{o}C for 10 minutes to dissolve. The temperature is monitored using a mercury-in-glass thermometer fitted with a clamp in the retort stand. Methanol was introduced, of which the quantity is 15 % w/w of the sample. The mixture was added concentrated sulphuric acid, which is 0.75 % w/w of the sample, and stirred using a magnetic hot plate at 55 to 60 ^{o}C in an open system for an hour. The mixture was transferred into a 500 ml separating funnel and allowed to separate overnight for 24 hours. It was separated into three phases: the lower phase, impurities; the middle phase, the preheated sample; and the upper layer, the methanol-water phase. The middle phase (oil) was collected and heated at 105 ^{o}C to remove excess moisture.

2.7 Transesterification procedure

In the presence of clay-doped BaCl, the shea butter oil and methanol reacted to form biodiesel and glycerol. The oil sample was quantitatively transferred on a hot magnetic stirrer and a flat-bottom flask. The needed quantity of methanol was reacted with the catalyst. The reaction was agitated throughout. The sample was removed at the predetermined time, allowed to cool, and the biodiesel and byproduct were separated by settling overnight at ambient conditions. The percentage of the biodiesel yield was determined using the formula in Equation 1.

$$\text{Yield (\%)} = \frac{\text{weight of methylester}}{\text{weight of oil used}} \times 100 \quad (1)$$

Table 1: Summary of the Experimental Factors Coding for the transesterification process

Factor	Units	Low level	Mid-low level	Mid-level	Mid-high level	High level
Catalyst conc(A)	Wt%	1(-2)	2(-1)	3(0)	4(+1)	5(+2)
Methanol/oil ratio, (B)	Mol/mol	4:1(-2)	6:1(-1)	8:1(0)	10:1(+1)	12:1(+2)
Time, (C)	Hour	1(-2)	1.5(-1)	2(0)	2.5(+1)	3(+2)
Temperature, (D)	°C	40(-2)	50(-1)	60(0)	70(+1)	80(+2)
Agitation speed(E)	RPM	150(-2)	200(-1)	250(0)	300(+1)	350(+2)

The five independent parameters (methanol/oil mole ratio, catalyst concentration, reaction temperature, reaction time, and agitation speed) were evaluated to investigate how they affected biodiesel yields. The experimental range and levels of the independent variables are shown in Table 1. Temperature, catalyst concentration, methanol/molar oil ratio, time, and agitation speed were independent variables for the optimization study. Biodiesel yield was selected as the response.

2.8 Genetic Algorithm (GA) Technique

A heuristic random search method called the Genetic Algorithm (GA) imitates the genetic process used by living things. The weakest people (chromosomes) and the most influential individuals, who often dominate the weakest, make up the process. Adhikesavan et al. (2002) state that people symbolize and genetically resemble reproductive chromosomes and factors. To address the optimization issue, GA offers a random search. It draws inspiration from the process of natural selection. It is a member of a broader family of evolutionary algorithms that employ biologically inspired operators like selection, crossover, and mutation to produce high-quality solutions for optimization and search problems. The fitness function is used to assess an individual's fitness, which is chromosome-dependent. At the beginning of the reproduction stage, individuals from the population are chosen and then recombined to produce offspring (Adhikesavan et al., 2021; Okpalaeke et al., 2020).

2.9 Performance Evaluation of the Developed Models

The assessment of the model for the transesterification process prediction was determined using the statistical parameters presented below:

(Mean square error) MSE = $\frac{1}{P}\sum_{p=1}^{p}(d_p - O_p)^2$ **(2)**

(Coefficient of determination) $R^2 = 1 - \frac{\sum_{p=1}^{p}(d_p - o_p)^2}{\sum_{p=1}^{p}(o_p)^2}$ **(3)**

$d_p$and o_p represent the desired and calculated outputs, respectively. The closeness of the MSE value to zero and the R^2 value to one depicts the models' efficiency (Sai et al., 2019; Oke et al., 2021)

3.0 RESULTS AND DISCUSSION

3.1 Physicochemical properties of shea butter oil

Table 2 shows the physiochemical properties of raw shea butter oil. The oils have moderate acid and free fatty acid values of 4.3828mgKOH/g and 2.1914% respectively. These values are high for one-step transesterification; hence, the oil must be pre-treated to avoid soap formation and ease glycerol separation. The saponification and peroxide values of the oil indicate that it is not prone to rancidity. The iodine value of shea butter oil (70.8I_2/100g) reveals the level of the unsaturated triglycerides present in oils. Both oils' densities and high viscosities will make their atomization difficult in internal combustion engines; hence, they cannot be used directly as bio-fuel (Sronsri et al., 2021). The oxidation stability of the oils was below ASTM D6751 standard (3 hours) for shea butter oil; this suggests further pretreatment for shea butter oil before utilization for the production of biodiesel. The high oxidation stability of the oils could result from the method used in extracting the oils (Abnisa et al., 2021). The kinematic viscosity compares favourably with reports from Ogaga et al. (2017) on palm kernel oil (57.34), showing that it is a potential feedstock with good fuel quality and that the oil is highly viscous and may tend to flow slowly.

Table 2: Physicochemical properties of oils

S/N	Physicochemical properties	Shea butter oil
1	Specific gravity	0.8935
2	Acid value (mgKOH/g)	4.3828
3	Free fatty acid (FFA) (%)	2.1914
4	Saponification value (mgKOH/g)	106.17

5	Iodine value (gI_2/100g)	70.85
6	Kinematic viscosity at 40°C (mm^2/s)	67.772
7	Peroxide value	5.95
8	Flash point	157
9	Cloud point	12.56
10	Pour point	10.89
11	Moisture content (%)	0.09
12	Refractive index	1.4646
13	Oxidation stability 110°C (Hour)	2.5
14	Molecular weight	744.3

3.2 Characterization of the oil

3.2.1 Fourier transform infra-red spectra of shea butter oil

In the spectrum of shea butter oil, 1006.4cm^{-1} corresponds to the C-O stretching vibration of the unsaturated fatty acid in the oil. The C-H methyl groups are indicated at 1259.8cm^{-1}. The aromatic contribution is found at the band 1748.1cm^{-1}. This peak confirms that shea butter comprises unsaturated fatty triglycerides for transesterification. More elaboration is seen in Figure 2 and Table 3. The observations are in tandem with the reports of Kuniyil et al. (2021) on waste cooking oil transesterification using ZnCuO/N-doped graphenenano composite as a catalyst and Ayoob et al. (2020) on biodiesel production from non-edible oil using a carbon-based catalyst synthesized from waste tires.

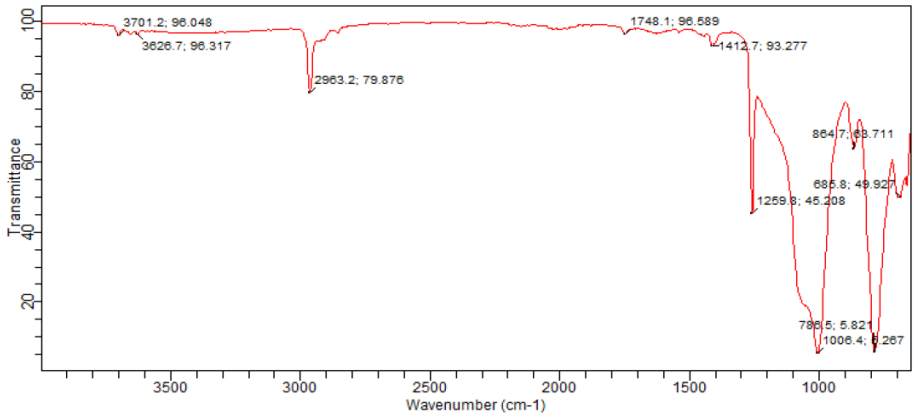

Figure 2: FTIR of raw shea butter oil

Table 3: The FT-IR spectrum of the raw shea butter oil

S/N	Group Frequency (cm^{-1}) Raw shea butter oil	Functional group/Assignment
1	685.8	=C-H Alkenes
2	1005.4	C-O, C-O-C stretching vibration, O-CH_3bending vibration
3	786.5	C-H methyl groups
4	1259.8	-C=C- bending vibration
5	1412.7	Aromatic combination
6	1748.1	O-H group stretched in a carboxylic acid
7	2963.2	Symmetric stretching vibrations of C-H alkane groups
8	3701.2	=C-H alkene group, C-H alkane

3.2.2 Fatty acid profile of SBO

Shea butter oil's fatty acid composition/profile was carried out using Gas Chromatography-Mass Spectrometry (GC-MS). The fatty acid composition is shown in Table 4. The oil showed an abundance of oleic acid (55.5wt%), Stearic acid (21.81wt%), Myristic acid (8.62wt%), and Linolenic acid (6.82wt%). The oil contains 38.59 wt.% saturated fatty acid and 62.32wt.% unsaturated fatty acid. The table shows that shea butter is the potential for transesterification based on its oleic and linolenic acid constituents(Qasemi et al., 2021; Taipabu et al., 2021; Yu et al., 2021).

Table 4: Fatty acid profile of shea butter oil for GCMS analysis

S/N	FFA Profile		Shea butter Oil
	Fatty Acid	Component	Composition (%)
1	Capric acid	C_{10}	1.72
2	Lauric acid	C_{12}	-
3	Myristic acid	C_{14}	8.62
4	Palmitic acid	$C_{16:0}$	5.8
5	Stearic acid	$C_{18:0}$	21.81
6	Oleic acid	$C_{18:1}$	55.5
7	Linoleic acid	$C_{18:2}$	-
8	Linolenic acid	$C_{18:3}$	6.82
9	Arachidic acid	C_{20}	0.64
	Total		100.91

3.3 Characterization of the synthesized catalyst

3.3.1 Physiochemical properties of the synthesized catalyst

The physical properties of the raw and modified clay catalysts are presented in Table 5; it could be observed that the properties of the clay improved after activation, with BaCl having more surface area. The pore size of the raw clay increased after different modes of activation. This may be attributed to the increased porosity of the synthesized material or the generation of secondary pores due to the linkage between BaCl. This agrees with the findings of Alaba et al.(2015) on the synthesis and application of mesoporous HZSM-5 for biodiesel production from shea butter and Olutoye et al. (2016) synthesis of fatty acid methyl esters via the transesterification of waste cooking oil by methanol with a barium-modified montmorillonite K10 catalyst.

Table 5: Physiochemical properties synthesized clay catalysts

Parameters	Raw clay	CDBaCl
Surface area (m^2/g)	284.286	258.924
Pore size (nm)	2.680	2.800
Total pore volume (cm^3/g)	24.11	24.46

3.3.2 FTIR of the clay-synthesized catalyst

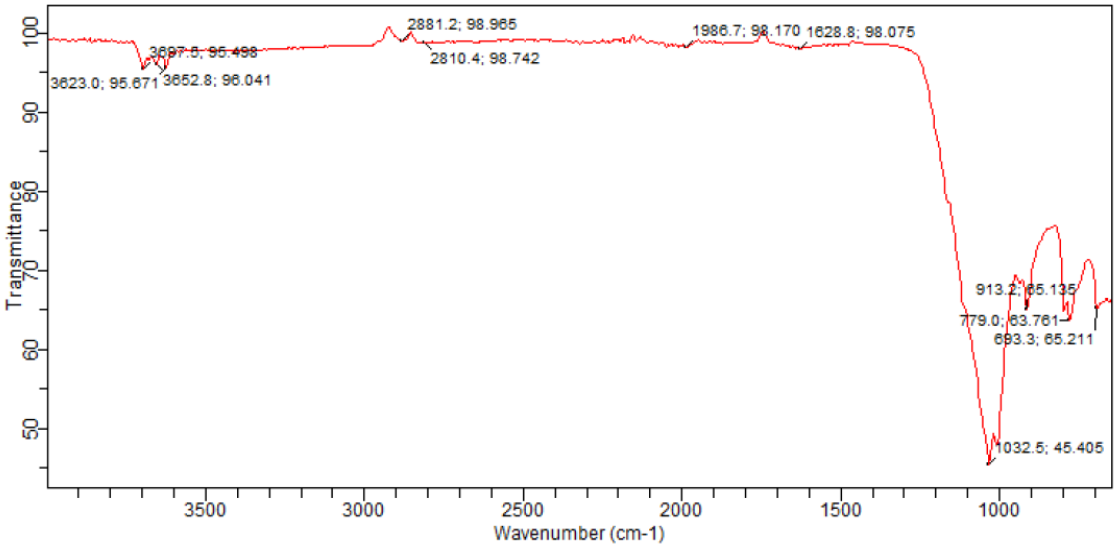

Figure 3: FTIR analysis of raw clay

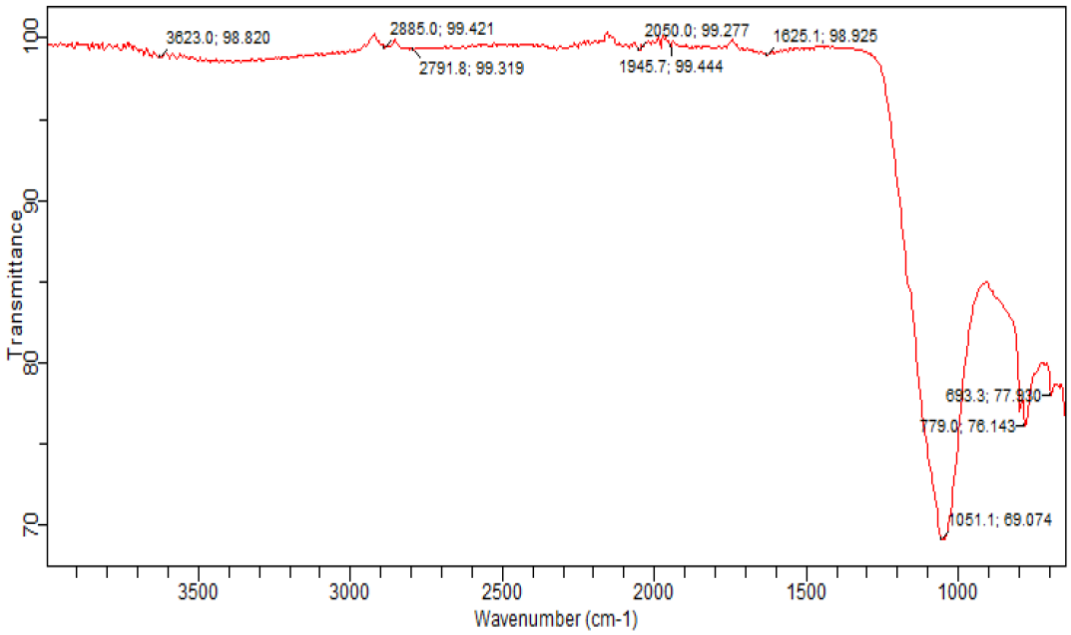

Figure 4: FTIR analysis of clay-doped BaCl

Fourier transform infrared (FTIR) spectroscopes of the raw clay catalyst, CD-BaCl,were done to ascertain their functional groups, as depicted in Figures 3 and 4. The results are also illustrated in Table 6. From the figures and table, it was observed that the catalysts have common functional groups such as Si-O-Si, C-Cl of aliphatic chloro compounds, C-H stretch of aromatic bend, C-H stretch of vinyl, Organic silicone Si-O-C, Si-O, double bond C=C, -OH stretch of primary alcohol and Al–OH–Al vibrations (Balajii & Niju, 2020). Comparing the raw clay to the CD-BaCl, it could be observed that there was no significant decrease in the intensity of bands at 693.3cm^{-1} for raw clay and CD-BaCl, suggesting that the structural changes attributed to the modifications are minor. The FTIR bands at 913.2cm^{-1} are attributed to Al–OH–Al for the raw clay (di Bitonto et al., 2020). These bands decreased in intensity after the

modification process due to the leaching of octahedral cations (Al^{3+}) from the clay structure(Rezania et al., 2021). The presence of free silica is corresponded to the Si–O–Si deformation (693.3 cm^{-1}) for raw clay and CD-BaCl catalyst and in-the-plane stretching of Si–O at wave numbers (1032.5 cm^{-1}) for raw clay, (1051.1 cm^{-1}) for CD-BaCl, The raw clay catalyst contains cyanide ion which can hinder the catalytic activity of the clay, but the modification of the clay with BaCl removed the cyanide content (Khan et al., 2020; Mazlita et al., 2016).

Table 6: FT-IR of the synthesized clay catalysts

S/N	Group Frequency (cm^{-1}) of catalyst Raw clay	CDBaCl	Functional group/Assignment
1	693.3	693.3	Si-O-Si deformation
2	779.0	779.0	Aliphatic chloro compounds, C-Cl
3	913.2	-	Aromatic C-H out-of-plane bend, Al-OH-Al
4	1032.5	1051.1	Organic siloxane/silicone (Si-O-C), Si-O
5	1628.8	1625.1	Conjugated ketone
6	1986.7	-	Cyanide ion
7	2881.2	2885.0	Double bond C = C, primary alcohol –OH stretch
8	3652.8	3623.0	Double bond C = C, primary alcohol –OH stretch

3.3.3 SEM analysis of the synthesized catalysts

The morphologies are shown in Figures 5 and 6, Micrographs of the clay catalyst samples synthesized by BaCl showed increased pores and pore size on the clay. Their morphology showed more agglomeration with a lack of morphological homogeny; more pore formation was observed in Figure 6, indicating increasing in porosity; the SEM observations conform with the findings of Salmasi et al. (2020) on the development of a novel K_2CO_3/Talc catalyst and Ude and Onukwuli, (2019) on the development of alkaline activated clay catalyst for the transesterification of oil from gmelina seed.

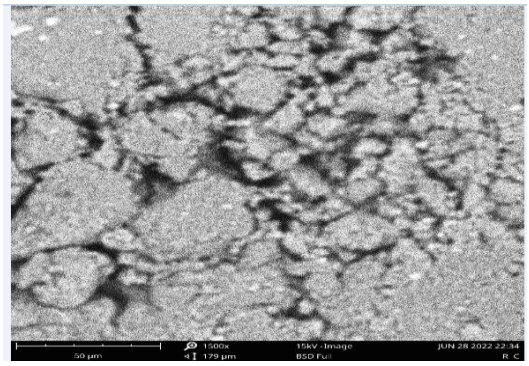

Figure 5: SEM of raw clay

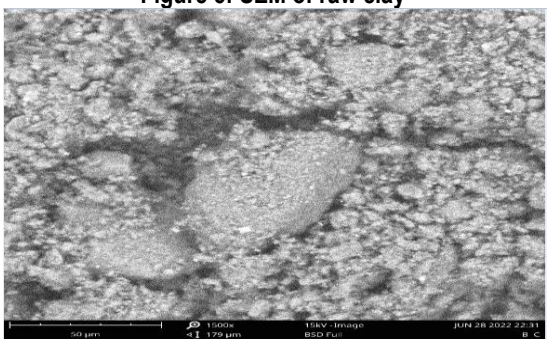

Figure 6: SEM of clay doped- BaCl

3.3.4 XRF analysis of the synthesized catalyst

Table 7 provides a summary of the chemical composition of the CD-BaCland raw clay that was employed in this investigation. Si, Al, Ti, and Fe comprise the clay's primary chemical compositions. It comprises metallic oxides that are components of heterogeneous catalysts, such as Al_2O_3, SiO_2, TiO_2, Cr_2O_3, Mn_2O_3, Fe_2O_3, and ZnO (Laskar et al., 2020; Varol et al., 2021). Clay exhibited high SiO_2 content; however, after being modified with BaCl, CD-BaCl showed a noticeable rise in BaO and Cl. SiO_2 was reduced when BaCl and ionic liquid were used to modify the raw clay. The modified clay was classified as Brønsted and Lewis acids by CD-BaCl, which also increased the amount of Al_2O_3 and Fe_2O_3. Thus, the activation increased the number and potency of Brønsted and Lewis acid sites. (Abdul Mutalib et al., 2020; Pavlović et al., 2020).

Table 7: X-ray fluorescence (XRF) of the synthesized catalysts

		Concentration (wt%)
Elements	**RC**	**CD-BaCl**
SiO_2	62.051	54.310
V_2O_5	0.189	0.3
Cr_2O_3	0.056	0.037
MnO	0.035	0.042
Fe_2O_3	3.971	4.5
CO_30_4	0.018	0.022
NiO	0.004	0.006
CuO	0.042	0.051
Nb_2O_3	0.034	0.041
SO_3	0.341	0.164
CaO	0.331	0.286
K_2O	0.228	0.196
BaO	0.130	4.190
Al_2O_3	27.323	28.751
Ta_2O_5	0.030	0.032
TiO_2	4.354	4.690
ZnO	0.009	0.188
Ag_2O	0.027	0.024
Cl	0.561	1.871
ZrO_2	0.265	0.299

3.3.5 XRD analysis of the synthesized catalyst

Figures 7 and 8 depict the XRD of the raw clay and CD-BaCl. The diffractogram displays a peak around 2θ = 27 ° for clay and 27.5° for CD-BaCl. The slight variations indicate that the raw clay was suitably modified with BaCl. Figure 6 demonstrates that the clay is a member of the kaolinite group, verifying the presence of alumina and silica and that it includes quartz. This residual clay identifies the origin of the clay. Illite, muscovite, and nacrite were found to be introduced when BaCl activated the clay; this may be attributed to the presence of BaCl involved in the modification (Bargole et al., 2021; Devaraj et al., 2019).

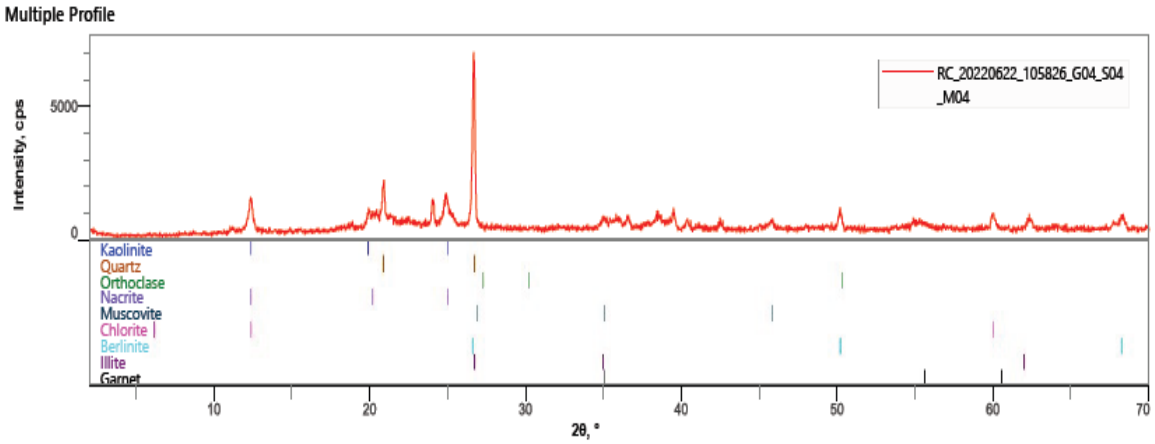

Figure 7: XRD analysis of the raw clay

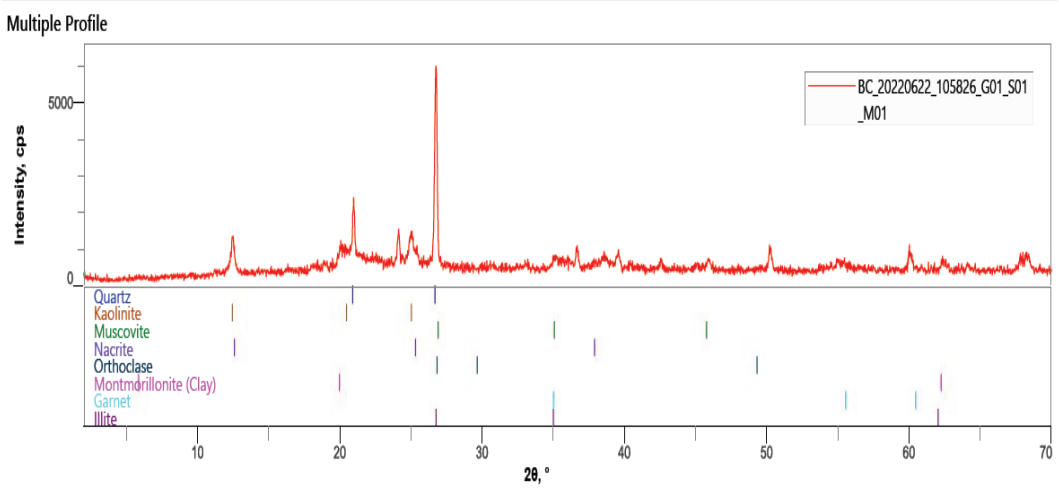

Figure 8: XRD analysis of the CD-BaCl

Table 8: Experimental run for CD-BaCl transesterification process using SBO

Run	A: Catalyst con.	B: methanol/oil ratio	C: time	D: temperature	E: Agitation speed	biodiesel yield
	wt %	mol/mol	hour	oC	rpm	%
1	2	6	2.5	70	400	87.22
2	4	6	2.5	50	400	70.22
3	3	8	2	60	500	81.23
4	3	4	2	60	300	73.35
5	3	8	3	60	300	75.52
6	4	6	2.5	70	200	75.24
7	4	10	1.5	70	200	68.74
8	2	10	2.5	70	200	74.35
9	2	6	1.5	50	400	79.55
10	1	8	2	60	300	76.99
11	3	8	2	60	300	70.22
12	3	8	2	60	300	70.22
13	4	10	2.5	70	400	85.37
14	2	10	1.5	50	200	86.8
15	3	8	2	60	300	70.22
16	4	10	1.5	50	400	73.82
17	2	6	2.5	50	200	63.21

18	3	8	2	60	300	70.22
19	3	8	2	40	300	60.58
20	5	8	2	60	300	73.12
21	2	10	2.5	50	400	64.51
22	2	10	1.5	70	400	81.52
23	4	6	1.5	50	200	68.59
24	4	6	1.5	70	400	70.49
25	3	12	2	60	300	80.81
26	3	8	2	60	300	70.22
27	3	8	2	60	300	70.22
28	3	8	1	60	300	75.55
29	4	10	2.5	50	200	76.76
30	3	8	2	80	300	67.33
31	3	8	2	60	100	75.93
32	2	6	1.5	70	200	68.04

Yield of SBO FAME by CD-BaCl = 70.2826 -0.987917 A + 1.84292B -0.0304167C + 1.70875 D + 1.73208 E + 0.686875AB + 3.28563AC -0.413125 AD -0.614375 AE - 1.19437BC -0.708125 BD -2.11438 BE + 4.21563 CD + 0.284375 CE + 2.84312 DE + 1.14614 A^2 + 1.65239 B^2 + 1.26614 C^2 -1.62886 D^2 + 2.02739 E^2 **(4)**

A quadratic polynomial was fitted to the presented data. The link between the biodiesel yield is described by equation4; the independent variables are (A) catalyst concentration, (B) methanol/oil molar ratio, (C) reaction temperature, (D) reaction time, and (E) agitation speed. RSM was used to predict the parameters through a transesterification reaction. Thirty-two experimental conditions were created using the Central Composite Design (CCD) to determine how the variable affected the response, as shown in Table 8. Several regression techniques were used to fit the coefficient of the quadratic polynomial regression mode of the response. (Latchubugata et al., 2018; Mostafa Marzouk et al., 2021; Taipabu et al., 2021).

Table 9: ANOVA for the model of biodiesel yield by CD-BaCl for shea butter oil

	Sum of		Mean	F	p-value	
Source	**Squares**	**df**	**Square**	**Value**	**Prob> F**	
Model	1310.73	20	65.54	285.09	< 0.0001	significant
A-catalyst con.	23.42	1	23.42	101.89	< 0.0001	
B-methanol/oil ratio	81.51	1	81.51	354.59	< 0.0001	
C-time	0.022	1	0.022	0.097	0.7618	
D-temperature	70.08	1	70.08	304.84	< 0.0001	
E-agitation speed	72.00	1	72.00	313.22	< 0.0001	
AB	7.55	1	7.55	32.84	0.0001	
AC	172.73	1	172.73	751.37	< 0.0001	
AD	2.73	1	2.73	11.88	0.0055	
AE	6.04	1	6.04	26.27	0.0003	
BC	22.82	1	22.82	99.29	< 0.0001	
BD	8.02	1	8.02	34.90	0.0001	
BE	71.53	1	71.53	311.16	< 0.0001	
CD	284.34	1	284.34	1236.92	< 0.0001	
CE	1.29	1	1.29	5.63	0.0370	
DE	129.33	1	129.33	562.61	< 0.0001	
A^2	38.53	1	38.53	167.62	< 0.0001	
B^2	80.09	1	80.09	348.40	< 0.0001	
C^2	47.02	1	47.02	204.56	< 0.0001	
D^2	77.83	1	77.83	338.56	< 0.0001	
E^2	120.57	1	120.57	524.49	< 0.0001	
Residual	2.53	11	0.23			

Lack of Fit	2.53	6	0.42		Not significant
Pure Error	0.000	5	0.000		
Cor Total	1313.26	31			
Std. Dev.	0.48		R-Squared	0.9981	
Mean	73.63		Adj R-Squared	0.9946	
C.V. %	0.65		Pred R-Squared	0.9499	
PRESS	65.77		Adeq Precision	68.866	

Table 9 indicates the analysis of variance results. The model's R^2, adjusted R^2, and predicted R^2 were 0.9981, 0.9946, and 0.9499, respectively, suggesting a good fit for the model and a good correlation between the observed and the predicted values. The overall model was statistically significant (p-value <0.05); the single, interaction, and quadratic terms are significant except for time, which is insignificant; this shows that all the process variables were consequential for shea butter oil transesterification. The standard deviation (0.48), mean (73.63), C.V% (0.65), and adequate precision (43.48539) indicate that the model is acceptable and robust for optimization. The lack of fit of the model (2.53), which is not significant, is suitable for the model. The findings agree with reports from Olatunji et al. (2021) on biodiesel yield transesterification from shea butter oil, Ajala et al. (2017) on the optimization of two stages of biodiesel production from shea butter oil, and Bastos et al. (2020) on the production of biodiesel using sulfonated catalyst from agro waste.

Table 10: Optimal response of the SBO biodiesel; RSM and GA comparison

Responses	Catalyst loading	Methanol/oil molar ratio	Time	Temperature	Agitation speed	Predicted yield
SBO catalyzed by CD-BaCl(RSM)	3.912	9.824	2.456	70	300	75.504
SBO catalyzed by CD-BaCl(GA)	3	12	3	50	208.8	81.49

Various process input factors, including catalyst loading, methanol/oil molar ratio, duration, temperature, and agitation speed, were optimized for the highest shear butter biodiesel production using RSM and GA algorithms. The projected ideal state for both approaches is displayed in Table 10. RSM had a lower yield (75.504%) than GA (81.49%). While the catalyst loading and time were almost the same as those predicted by RSM, GA significantly reduced the temperature and agitation speed, making it superior to RSM for optimization (Okpalaeke et al., 2020; Suresh et al., 2021).

Table 11: Shea butter biodiesel characterization (optimal yield) ASTM standards

Physicochemical properties	Shea butter biodiesel	ASTM D6751
Free fatty acid value (mgKOH/g)	0.21	
Iodine value (gI_2/100g)	3.09	
Cetane number	47.5	min- 47
Gross calorific value (J/g)	7215.1	
Kinematic viscosity @ 40^{o}C (mm2s-1)	4.25	1.9-60
Specific gravity	0.917	
Flashpoint (^{o}C)	171	min- 130
Moisture (%)	0.011	
Cloud point (^{o}C)	9.12	-15 to 15
Acid value (mg KOH/g)	0.42	Max 0.5

The physical and chemical characteristics of the biodiesel made from the oil are shown in Table 11. The biodiesel has a moisture content of 0.011% and a specific gravity of 0.917, which is within the acceptable range. The iodine value of 3.09 denotes the transesterification of unsaturated fatty acid triglycerides. The biodiesel acid (0.42) and free fatty acid value (0.21) produced were within the ASTM specification for biodiesel, protecting the fuel from corrosion and deposits on the engine. The delay interval is shorter, and the fuel is more combustible with a higher cetane number. Low cetane fuels make it challenging to start the engine and cause smoke. The cetane number

(47.5), which is higher than the ASTM limit (47 indicates that the biodiesel has low emission and clean combustion, attributed to the nature of the catalyst used during the transesterification process. Other properties, such as flash point, cloud point, and gross calorific value of theshea butteroil biodiesel, were within ASTM limits for biodiesel. The kinematic viscosity (4.25 mm^2/s) is within the ASTM limits (1.9-6.0) indicates that the biodiesel can flow freely (Nadeem et al., 2021; Tamoradi et al., 2021).

CONCLUSION

The comparative performance of RSM and GA to predict shea butter transesterification via CD-BaCl as a heterogeneous catalyst was evaluated in this work. The synthesized catalyst was characterized using FT-IR, SEM, XRF, XRD, and BET to confirm its activation for the transesterification process. The 3D and ANOVA affirmed that the process parameters significantly impacted the process. The results demonstrated that GA performed better than RSM with higher biodiesel yield and reduced process parameters to ensure a cost-effective process. The properties of the shea butter biodiesel met the ASTM D6751 standards specifications.

References

A. V. S. L. Sai, B., Niju, S., K. M. Meera, B., and Anantharaman, N. (2019). Optimization and modelling of biodiesel production using fluorite as a heterogeneous catalyst. *Energy Sources, Part A: Recovery, Utilization and Environmental Effects*, *41*(15), 1862–1878. https://doi.org/10.1080/15567036.2018.1549165

Abdul Mutalib, A. A., Ibrahim, M. L., Matmin, J., Kassim, M. F., Mastuli, M. S., Taufiq-Yap, Y. H., Shohaimi, N. A. M., Islam, A., Tan, Y. H., and Kaus, N. H. M. (2020). SiO2-Rich Sugar Cane Bagasse Ash Catalyst for Transesterification of Palm Oil. *Bioenergy Research*, *13*(3), 986–997. https://doi.org/10.1007/s12155-020-10119-6

Abnisa, F., Sanni, S. E., and Alaba, P. A. (2021). Comparative study of catalytic performance and degradation kinetics of biodiesels produced using heterogeneous catalysts from kaolinite. *Journal of Environmental Chemical Engineering*, *9*(4), 105569. https://doi.org/10.1016/j.jece.2021.105569

Adhikesavan, C., Balamurugan, C., & Ganesh, D. (2021). *Application of Genetic Algorithm for Increasing the Utilization of Poor-quality Biodiesel through Blending*. *1050*(8), 1039–1050.

Alaba, P.A., Sani, Y.M., Mohammed, I.Y., Abakr, Y. A., & Daud, W. M. A. W. (2015). synthesis and application of hierarchical mesoporous HZSM-5 for biodiesel production from shea butter. J*ournal of the Taiwan Insitute of Chemical Engineers*. 000, 1-8.

Ajala, E O, Olaniyan, A. M., Aberuagba, F., Ajala, M. A., Odewole, M. M., Olaniyan, A. M., Aberuagba, F., Ajala, M. A., & Odewole, M. M. (2018). One-pot synthesis of biodiesel from high FFA shea butter in an optimisation study using response surface methodology. *Biofuel*, *7269*. https://doi.org/10.1080/17597269.2017.1416523

Ayoob, A. K., & Fadhil, A. B. (2020). Valorization of waste tires in the synthesis of an effective carbon based catalyst for biodiesel production from a mixture of non-edible oils. *Fuel*, *264*, 116754. https://doi.org/10.1016/j.fuel.2019.116754

Balajii, M., and Niju, S. (2020). Banana peduncle – A green and renewable heterogeneous base catalyst for biodiesel production from Ceiba pentandra oil. *Renewable Energy*, *146*, 2255–2269. https://doi.org/10.1016/j.renene.2019.08.062

Bambase, M. E., Almazan, R. A. R., Demafelis, R. B., Sobremisana, M. J., and Dizon, L. S. H. (2021). Biodiesel production from refined coconut oil using hydroxide-impregnated calcium oxide by cosolvent method. *Renewable Energy*, *163*, 571–578. https://doi.org/10.1016/j.renene.2020.08.115

Bargole, S. S., Singh, P. K., George, S., & Saharan, V. K. (2021). Valorization of low fatty acid content waste cooking oil into biodiesel through transesterification using a basic heterogeneous calcium-based catalyst. *Biomass and Bioenergy*, *146*(February), 105984. https://doi.org/10.1016/j.biombioe.2021.105984

Bastos, R. R. C., da Luz Corrêa, A. P., da Luz, P. T. S., da Rocha Filho, G. N., Zamian, J. R., & da Conceição, L. R. V. (2020). Optimization of biodiesel production using sulfonated carbon-based catalyst from an amazon agro-industrial waste. *Energy Conversion and Management*, *205*, 112457. https://doi.org/10.1016/j.enconman.2019.112457

Dadhania, H., Raval, D., and Dadhania, A. (2021). Magnetically separable heteropolyanion-based ionic liquid as a heterogeneous catalyst for ultrasound-mediated biodiesel production through the esterification of fatty acids. *Fuel*, *296*(March), 120673. https://doi.org/10.1016/j.fuel.2021.120673

Dai, Y. M., Li, Y. Y., Lin, J. H., Kao, I. H., Lin, Y. J., and Chen, C. C. (2021). Applications of M2ZrO2 (M = Li, Na, K) composite as a catalyst for biodiesel production. *Fuel*, *286*(May 2020), pp. 1–7. https://doi.org/10.1016/j.fuel.2020.119392

Devaraj, K., Veerasamy, M., Aathika, S., Mani, Y., Thanarasu, A., Dhanasekaran, A., and Subramanian, S. (2019). Study on effectiveness of activated calcium oxide in pilot plant biodiesel production. *Journal of Cleaner Production*, *225*, 18–26. https://doi.org/10.1016/j.jclepro.2019.03.244

di Bitonto, L., Reynel-Ávila, H. E., Mendoza-Castillo, D. I., Bonilla-Petriciolet, A., Durán-Valle, C. J., and Pastore, C. (2020). Synthesis and characterization of nanostructured calcium oxides supported onto biochar and their application as catalysts for biodiesel production. *Renewable Energy*, *160*, 52–66. https://doi.org/10.1016/j.renene.2020.06.045

Esonye, C., Onukwuli, O. D. & Ofoefule, U. A. (2019). Industrial Crops & Products Characterization and oxidation modeling of oils from *Prunus amygdalus* , *Dyacrodes edulis and Chrysophyllum albidium*. *Industrial Crops & Products*, *128*, 298–307. https://doi.org/10.1016/j.indcrop.2018.11.029

Jalalmanesh, S., Kazemeini, M., Rahmani, M. H., and Zehtab Salmasi, M. (2021). Biodiesel Production from Sunflower Oil Using K2CO3 Impregnated Kaolin Novel Solid Base Catalyst. *JAOCS, Journal of the American Oil Chemists' Society*, *98*(6), 633–642. https://doi.org/10.1002/aocs.12486

Kuniyil, M., Shanmukha Kumar, J. V., Adil, S. F., Assal, M. E., Shaik, M. R., Khan, M., Al-Warthan, A., & Siddiqui, M. R. H. (2021). Production of biodiesel from waste cooking oil using ZnCuO/N-doped graphene nanocomposite as an efficient heterogeneous catalyst. *Arabian Journal of Chemistry*, *14*(3), 102982. https://doi.org/10.1016/j.arabjc.2020.102982

Laskar, I. B., Gupta, R., Chatterjee, S., Vanlalveni, C., & Rokhum, L. (2020). Taming waste: Waste *Mangiferaindica* peel as a sustainable catalyst for biodiesel production at room temperature. *Renewable Energy*, *161*, 207–220. https://doi.org/10.1016/j.renene.2020.07.061

Latchubugata, C. S., Kondapaneni, R. V., Patluri, K. K., Virendra, U., & Vedantam, S. (2018). Kinetics and optimization studies using response surface methodology in biodiesel production using heterogeneous catalyst. *Chemical Engineering Research and Design*, *135*, 129–139. https://doi.org/10.1016/j.cherd.2018.05.022

Lim, S., Yap, C. Y., Pang, Y. L., and Wong, K. H. (2020). Biodiesel synthesis from oil palm empty fruit bunch biochar derived heterogeneous solid catalyst using 4-benzene diazonium sulfonate. *Journal of Hazardous Materials*, *390*, 121532. https://doi.org/10.1016/j.jhazmat.2019.121532

Khan, H., Iqbal, T., Haider Ali, C., Javaid, A., and Iqbal Cheema, I. (2020). Sustainable biodiesel production from waste cooking oil utilizing waste ostrich (Struthio camelus) bones derived heterogeneous catalyst. *Fuel*, *277*(April), 118091. https://doi.org/10.1016/j.fuel.2020.118091

Mazlita, Y., Lee, H. V., and Hamid, S. B. A. (2016). Preparation of cellulose nanocrystals bio-polymer from agro-industrial wastes: Separation and characterization. *Polymers and Polymer Composites*, *24*(9), 719–728. https://doi.org/10.1177/096739111602400907

Mostafa Marzouk, N., Abo El Naga, A. O., Younis, S. A., Shaban, S. A., El Torgoman, A. M., and El Kady, F. Y. (2021). Process optimization of biodiesel production via esterification of oleic acid using sulfonated hierarchical mesoporous ZSM-5 as an efficient heterogeneous catalyst. *Journal of Environmental Chemical Engineering*, *9*(2), 105035. https://doi.org/10.1016/j.jece.2021.105035

Nadeem, F., Bhatti, I. A., Ashar, A., Yousaf, M., Iqbal, M., Mohsin, M., Nisar, J., Tamam, N., and Alwadai, N. (2021). Eco-benign biodiesel production from waste cooking oil using eggshell derived MM-CaO catalyst and condition optimization using RSM approach. *Arabian Journal of Chemistry*, *14*(8), 103263. https://doi.org/10.1016/j.arabjc.2021.103263

Naveenkumar, R., and Baskar, G. (2021). Process optimization, green chemistry balance, and techno-economic analysis of biodiesel production from castor oil using heterogeneous nanocatalyst. *Bioresource Technology*, *320*, 124347. https://doi.org/10.1016/j.biortech.2020.124347

Nazir, M. H., Ayoub, M., Zahid, I., Shamsuddin, R. Bin, Yusup, S., Ameen, M., Zulqarnain, and Qadeer, M. U. (2021). Development of lignin-based heterogeneous solid acid catalyst derived from sugarcane bagasse for microwave assisted-transesterification of waste cooking oil. *Biomass and Bioenergy*, *146*(December 2020), 105978.

https://doi.org/10.1016/j.biombioe.2021.105978

Nisar, S., Hanif, M. A., Rashid, U., Hanif, A., Akhtar, M. N., & Ngamcharussrivichai, C. (2021). Trends in widely used catalysts for fatty acid methyl esters (Fame) production: A review. *Catalysts*, *11*(9). https://doi.org/10.3390/catal11091085

Ogaga, B., Adeleke, I. A., Damos, M., Adeola, H., Ernest, K., & Betiku, E. (2017). Optimization of biodiesel production from *Thevetiaperuviana* seed oil by adaptive neuro-fuzzy inference system coupled with genetic algorithm and response surface methodology. *Energy Conversion and Management*, *132*, 231–240.

Oke, E. O., Adeyi, O., Okolo, B. I., Ude, C. J., Adeyi, J. A., Salam, K. K., Nwokie, U., and Nzeribe, I. (2021). Heterogeneously catalyzed biodiesel production from Azadiricha Indica oil: Predictive modelling with uncertainty quantification, experimental optimization, and techno-economic analysis. *Bioresource Technology*, *332*(April), 125141. https://doi.org/10.1016/j.biortech.2021.125141

Onukwuli, O. D., & Ude, C. N. (2018). Kinetics of African pear seed oil (APO) methanolysis catalyzed by phosphoric acid - activated kaolin clay. *Applied Petrochemical Research*, *8*(4), 299–313. https://doi.org/10.1007/s13203-018-0210-0

Okpalaeke, K. E., Ibrahim, T. H., Latinwo, L. M., and Betiku, E. (2020). *Mathematical Modeling and Optimization Studies by Arti fi cial Neural Network, Genetic Algorithm and Response Surface Methodology : A Case of Ferric Sulfate – Catalyzed Esteri fi cation of Neem (Azadirachta indica) Seed Oil*. *8*(November), 1–14. https://doi.org/10.3389/fenrg.2020.614621

Olatunji, O. M., Horsfall, I. T., & Ubom, E. V. (2021). Response surface optimization approach to predict the maximum % biodiesel yield via transesterification of esterified shea butter oil. *Current Research in Green and Sustainable Chemistry*, *4*, 100167. https://doi.org/10.1016/j.crgsc.2021.100167

Olutoye, M. A., Wong, S. W., Chin, L. H., Amani, H., Asif, M., & Hameed, B. H. (2016). Synthesis of fatty acid methyl esters via the transesterification of waste cooking oil by methanol with a barium-modified montmorillonite K10 catalyst. *Renewable Energy*, *86*, 392-398.

Pavlović, S. M., Marinković, D. M., Kostić, M. D., Janković-Častvan, I. M., Mojović, L. V., Stanković, M. V., and Veljković, V. B. (2020). A CaO/zeolite-based catalyst obtained from waste chicken eggshell and coal fly ash for biodiesel production. *Fuel*, *267*(September 2019), 117171. https://doi.org/10.1016/j.fuel.2020.117171

Qasemi, Z., Jafari, D., Jafari, K., & Esmaeili, H. (2021). Heterogeneous aluminium oxide/calcium oxide catalyzed transesterification of Mespilus germanica triglyceride for biodiesel production. *Environmental Progress and Sustainable Energy*, *August*, pp. 1–12. https://doi.org/10.1002/ep.13738

Rezania, S., Kamboh, M. A., Arian, S. S., Al-Dhabi, N. A., Arasu, M. V., Esmail, G. A., and Kumar Yadav, K. (2021). Conversion of waste frying oil into biodiesel using recoverable nanocatalyst based on magnetic graphene oxide supported ternary mixed metal oxide nanoparticles. *Bioresource Technology*, *323*(December 2020), 124561. https://doi.org/10.1016/j.biortech.2020.124561

Sahu, O. (2021). Characterization and utilization of heterogeneous catalyst from waste rice-straw for biodiesel conversion. *Fuel*, *287*(May), 119543. https://doi.org/10.1016/j.fuel.2020.119543

Salmasi, M. Z., Kazemeini, M., and Sadjadi, S. (2020). Transesterification of sunflower oil to biodiesel fuel utilizing a novel K2CO3/Talc catalyst: Process optimizations and kinetics investigations. *Industrial Crops and Products*, *156*(May). https://doi.org/10.1016/j.indcrop.2020.112846

Sronsri, C., Sittipol, W., and U-yen, K. (2021). Performance of CaO catalyst prepared from magnetic-derived CaCO3 for biodiesel production. *Fuel*, *304*(July), 121419. https://doi.org/10.1016/j.fuel.2021.121419

Suresh, T., Sivarajasekar, N., & Balasubramani, K. (2021). Enhanced ultrasonic assisted biodiesel production from meat industry waste (pig tallow) using green copper oxide nanocatalyst: Comparison of response surface and neural network modelling. *Renewable Energy*, *164*, 897–907. https://doi.org/10.1016/j.renene.2020.09.112

Taipabu, M. I., Viswanathan, K., Wu, W., and Nagy, Z. K. (2021). Production of renewable fuels and chemicals from fats, oils, and grease (FOG) using homogeneous and heterogeneous catalysts: Design, validation, and optimization. *Chemical Engineering Journal*, *424*(May), 130199. https://doi.org/10.1016/j.cej.2021.130199

Tamoradi, T., Kiasat, A. R., Veisi, H., Nobakht, V., Besharati, Z., & Karmakar, B. (2021). MgO doped magnetic graphene derivative as a competent heterogeneous catalyst producing biofuels via transesterification: Process optimization through Response Surface Methodology (RSM). *Journal of Environmental Chemical Engineering*, *9*(5), 106009. https://doi.org/10.1016/j.jece.2021.106009

Ude, C. N., &Onukwuli, O. D. (2019). Kinetic modeling of transesterification of gmelina seed oil catalyzed by alkaline activated clay (NaOH/clay) catalyst. *Reaction Kinetics, Mechanisms and Catalysis*, *127*, 1039-1058.

Varol, P. M., Çakan, A., Kiren, B., & Ayas, N. (2021). Microwave-assisted catalytic transesterification of soybean oil using KOH/γ-Al2O3. *Biomass Conversion and Biorefinery*. 13 (1), 633-645. https://doi.org/10.1007/s13399-020-01253-4

Yatish, K. V., Prakash, R. M., Ningaraju, C., Sakar, M., GeethaBalakrishna, R., and Lalithamba, H. S. (2021). Terminalia chebula is a novel green source for the synthesis of copper oxide nanoparticles and as feedstock for biodiesel production and its application on diesel engines. *Energy*, *215*, 119165. https://doi.org/10.1016/j.energy.2020.119165

Yu, H., Cao, Y., Li, H., Zhao, G., Zhang, X., Cheng, S., & Wei, W. (2021). An efficient heterogeneous acid catalyst derived from a waste ginger straw for biodiesel production. *Renewable Energy*, pp. *176*, 533–542. https://doi.org/10.1016/j.renene.2021.05.098

Yusuff, A. S., Bhonsle, A. K., Bangwal, D. P., &Atray, N. (2021). Development of a barium-modified zeolite catalyst for biodiesel production from waste frying oil: Process optimization by design of Experiment. *Renewable Energy*, *177*, 1253-1264.